2020

Nitrite admixed concrete for wastewater structures: Mechanical properties, leaching behavior and biofilm development

Xuan Li
University of Queensland

Liza O'Moore
University of Queensland

Simeon Wilkie
University of Queensland, Getty Conservation Institute

Yarong Song
University of Queensland

Jing Wei
University of Queensland

See next page for additional authors

Nitrite admixed concrete for wastewater structures: Mechanical properties, leaching behavior and biofilm development

Abstract

This study systematically investigated the impacts of calcium nitrite addition on the mechanical properties and biofilm communities of concrete-based wastewater infrastructures using sulfate resistant cement through standard tests and DNA sequencing, respectively. The results revealed that setting time and water demand for normal consistency were reduced, but slump, drying shrinkage, and apparent volume of permeable voids increased with calcium nitrite dosage up to 4% weight of cement. The cumulative leached fraction of nitrite, 28-day compressive strength and biofilm communities were not significantly affected by calcium nitrite dosages. The addition of calcium nitrite into concrete is environmentally friendly to wastewater infrastructures.

Disciplines

Engineering | Science and Technology Studies

Publication Details

Li, X., O'Moore, L., Wilkie, S., Song, Y., Wei, J., Bond, P. L., Yuan, Z., Hanzic, L. & Jiang, G. (2020). Nitrite admixed concrete for wastewater structures: Mechanical properties, leaching behavior and biofilm development. Construction and Building Materials, 233 117341-1-117341-9.

Authors

Xuan Li, Liza O'Moore, Simeon Wilkie, Yarong Song, Jing Wei, Philip Bond, Zhiguo Yuan, Lucija Hanzic, and Guangming Jiang

Nitrite admixed concrete for wastewater structurers: mechanical properties, leaching behavior and biofilm development

Xuan Li [a], Liza O'Moore [b], Simeon Wilkie [a, c], Yarong Song [a], Jing Wei [a], Philip L. Bond [a], Zhiguo Yuan [a], Lucija Hanzic [b], Guangming Jiang [a, d, *]

[a] Advanced Water Management Centre, the University of Queensland, Australia

[b] School of Civil Engineering, the University of Queensland, Australia

[c] Getty Conservation Institute, Los Angeles, USA

[d] School of Civil, Mining and Environmental Engineering, University of Wollongong, Australia

XL: xuan.li@awmc.uq.edu.au; LO: l.omoore@uq.edu.au SW: swilkie@getty.edu

YS: yarong.song @awmc.uq.edu.au PB: p.bond@uq.edu.au; ZY: z.yuan@awmc.uq.edu.au

* Corresponding author. E-mail: gjiang@uow.edu.au; g.jiang@awmc.uq.edu.au; Tel.: +61 02 4221 3792.

Highlights:

- A systematical study of the impact of calcium nitrite addition in sewer structures
- Mechanical property changes in concrete is proportional to calcium nitrite dosages
- Concrete with up to 4% calcium nitrite meets the structural requirement
- Nitrite leached to receiving water is proportional to the level of addition
- Calcium nitrite in concrete is environmentally friendly to anaerobic sewer biofilms

Abstract:

This study systematically investigated the impacts of calcium nitrite addition on the mechanical properties and biofilm communities of concrete-based wastewater infrastructures using sulfate resistant cement through standard tests and DNA sequencing, respectively. The results revealed that setting time and water demand for normal consistency were reduced, but slump, drying shrinkage, and apparent volume of permeable voids increased with calcium nitrite dosage up to 4% weight of cement. The cumulative leached fraction of nitrite, 28-day compressive strength and biofilm communities were not significantly affected by calcium nitrite dosages. The addition of calcium nitrite into concrete is environmentally friendly to wastewater infrastructures.

Keywords: Calcium nitrite, Concrete, Corrosion, Sewer, Biofilm, Sulfate resistant cement

1. Introduction

Civil infrastructure systems, such as sewer networks, are critical and essential parts of modern societies. With socio-economic development and population growth, the demand for such infrastructure has increased greatly. To ensure the durability and reliability of the sewer infrastructure, steel-reinforced concrete is widely applied due to its high compressive and tensile strength [1]. However, significant deterioration caused by sulfate attack, chloride penetration and biodeterioration commonly occurs in the structures subject to aggressive environments and can ultimately lead to early structural failure [2, 3].

Wastewater infrastructures, including sewer networks and wastewater treatment plants, are often exposed to aggressive environments. Sourced from sewage, sulfate attacks concrete infrastructures that are fully or partially submerged in sewage [4]. In submerged parts of infrastructures, sulfate from sewage attacks the cementitious paste of the concrete through direct contact forming ettringite and gypsum. These reactions are high expansive and cause the cracking and disintegration of the concrete [5]. In partially submerged structures, such as in gravity sewers, sulfate in sewage can be transformed into hydrogen sulfide and released into sewer gas. In the sewer the high moisture, microbial inoculation and supply of nutrients coming from wastewater, provide favorable conditions for the biological sulfide oxidation and acid production [6]. Subsequently, H_2S in sewer gas is oxidized into sulfuric acid on the concrete surface and attacks the concrete above the water level [7]. Both the sulfate attack from wastewater and sulfuric acid form on the concrete surface produces expansive corrosion products, and weakens the structural capacity [8]. Iron in the concrete facilitates the development of cracks along the corrosion front, and enhances the erosion of the concrete protection layer [9]. Due to the expansive corrosion products and cracks, water and oxygen availabilities to the steel increase significantly, which further accelerates the corrosion of the rebar steel [10, 11]. In most of the countries, sulfate resistant cement is required to be used for sewer manufacture due to the exposure environment [12] [13]. Fly ash, a type of pozzolan, is a common admixture in sulfate resistant cement [14]. The addition of fly ash in cement reduces the calcium hydroxide content and permeability of concrete, which increases the resistance of concrete to the attack from sulfate [15].

In addition to sulfate attack, chloride ingress is another major cause of the rebar steel corrosion [16]. Penetrating through cracks or pore structures in concrete, chloride reaches the steel and depassivates the protective layer of steel. After the depassivation, steel corrosion initiates and produces expansive corrosion products, i.e. iron rust. Similar to the sulfate attack, the expansive corrosion products induce the cracking process and accelerate the steel corrosion [4]. Chloride is ubiquitous in sewage and it can be at very high levels when the residual chloride from the application of de-icing agents enters into sewers in winters [2]. Furthermore, some coastal cities (e.g. Hong Kong) have very high chloride in the wastewater system due to the use of seawater for toilet flushing [17]. Therefore, the ingress of sulfate and chloride causes a combination of rebar corrosion and concrete cracking, resulting in the accelerated deterioration of concrete-based wastewater infrastructures [2].

Calcium nitrite has been widely used as a corrosion inhibitor against chloride attack of rebar steel for several decades [18]. Calcium nitrite increases the chloride threshold level and also the corrosion-free life of concrete [19]. However, the addition of calcium nitrite is reported to change the physical and mechanical properties of concrete. Calcium nitrite accelerates the formation of calcium hydroxide and increases the total volume of pore structures in concrete, which weakens the resistance of concrete to sulfate attack [20]. The addition of calcium nitrite in ordinary Portland cement (OPC) usually increases the air content, the workability of fresh concrete and the cumulative pore volume of hardened concrete. Nitrite is reported to affect the compressive strength of the concrete positively or negatively depending on different mix designs [21-23]. However, there is no report on the impacts of admixing calcium nitrite with sulfate resistant cement on the properties of concrete. To investigate the feasibility of adding calcium nitrite as an admixture into sulfate resistant cement for wastewater structures, it is essential to understand the changes in fresh and mechanical properties under different calcium nitrite levels.

Inevitably, sewage structures are fully or partially submerged in wastewater. Leaching of nitrite into wastewater is thus a major concern for sewage structures using nitrite-admixed concrete. A sufficient level of nitrite in concrete is a key factor for achieving the inhibitory effect on steel corrosion [24]. A previous study using OPC found that the leaching behavior of nitrite is affected by the curing time, mix design and temperature [25]. The leaching behavior of nitrite admixed with sulfate resistant cement at different dosages has not been investigated.

Furthermore, biofilms develop on the concrete surface in the sewer system and downstream wastewater treatment facilities [26]. Nitrite-admixed concrete may affect the wastewater biofilms due to the inhibitory effects of nitrite on microorganisms. Depending on the pH and nitrite concentration, inhibitory and biocidal effects are observed on sulfate-reducing bacteria (SRB) and methanogens in anaerobic sewer biofilms, and on ammonia-oxidizing bacteria and polyphosphate-accumulating organisms in the wastewater treatment process [27]. These effects may be desired or undesired for the benefit of wastewater management. Regardless, it is necessary to understand the potential impact of nitrite admixed with sulfate resistant cement on the activity and development of biofilms in wastewater.

Collectively speaking, this study aims to investigate the impact of calcium nitrite and its dosages as an admixture with sulfate resistant cement on the fresh and hardened concrete properties, the nitrite leaching behavior and the biofilms on the concrete surface. Five different dosages of calcium nitrite were employed to cast test specimens. The relationship between the concrete properties and nitrite dosages was determined and analyzed with regression models. Nitrite leaching performance was tested for three different calcium nitrite dosages over 15 months. Laboratory-scale anaerobic wastewater reactors were used to monitor the development of biofilms on the nitrite-admixed concrete with three different dosages in real domestic sewage over six months. This systematical investigation will support the development and application of nitrite-admixed concrete for durable, resilient and sustainable wastewater infrastructures.

2. Materials and methods

2.1 Ingredients and mix design

General Blended sulfate-resistant cement (Cement Australia Builders Cement), in compliance with AS 3972 [28] was adopted as the primary binder in this study. This cement contains 75–95% of Portland cement clinker, 5–25% fly ash and 0–5% minor additional constituents.

The coarse aggregates were crushed aggregate (CA) with a nominal maximum particle size of 10 mm, specific gravity (SG) of 2.89, fineness modulus of 4.17, and water absorption (A) of 0.28%. Three fine aggregates including crushed manufactured sand (MS), natural river sand (RS) and natural fine sand (FS) have a specific gravity of 2.91, 2.67 and 2.66, fineness modulus of 4.82, 7.26 and 8.94, water absorption of 0.56%, 2.41% and 1.61%, respectively.

A conventional concrete mix design (industrial based), typically used in sewer pipes for sulfate exposure class, was adopted in this study (Table 1). A water/cement (w/c) ratio of 0.4 was used in all the mixes. The key parameter examined experimentally was the dosage of calcium nitrite by weight (0%, 1%, 2%, 3%, 4% of cement weight). Calcium nitrite ($Ca(NO_2)_2$) solution (30 wt. % in H_2O, Sigma-Aldrich) was applied according to the mix design (Table 1). Polycarboxylate ether polymers superplasticiser (MasterGlenium SKY 8700, BASF) was added to achieve the desired workability (Table 1).

Table 1 Summary of mix designs used for concrete properties study

Calcium nitrite dosage	Constituents (kg/m^3)									
	w/c	Cement	Free water	$Ca(NO_2)_2$	Aggregates [a]					S.P.[b]*(l)*
					10mm	MS	RS	FS	TOTAL	
0%	0.4	420	168	0	750	375	469	281	1876	4.2
1%	0.4	420	168	4.2	749	374	468	281	1871	4.2
2%	0.4	420	168	8.4	747	373	467	280	1867	4.2
3%	0.4	420	168	12.6	745	372	466	279	1862	4.2
4%	0.4	420	168	16.8	743	372	464	279	1858	4.2

[a] In aggregates, 10mm, MS, RS, FS are the coarse aggregates, manufactured sand, natural river sand and natural fine sand, respectively.

[b] S.P.: superplasticizer.

2.2 Mixing, casting and curing procedure

Concrete mixing was carried out in accordance with AS 1012.2 [29], in a conforming revolving pan mixer (Bennet 70L laboratory mixer). The mixing procedure was as follows: firstly, the coarse aggregate followed by the fine aggregate were hand loaded into the concrete mixer with a sufficient quantity of mixing water (approximately 50%) and mixed for 30 seconds. Then cement was added and covered with some of the aggregates. After that, the ingredients were mixed for 2 minutes and the remaining mix water and admixture (calcium nitrite and superplasticisers) were added within the first minute of mixing. After mixing, the mixer was stopped to rest for 2 minutes and operated for a further 2 minutes. The slump was measured within 3 minutes of stopping the mixer (section 2.3.2). After slump measurement, another 2 minutes of mixing was applied and then the fresh mixtures were filled into the molds for compressive strength measurements (section 2.3.3), drying shrinkage measurements (section 2.3.4) and apparent volume of permeable voids measurements (section 2.3.5). The mixture was consolidated on a vibration table within the next 20 minutes. Immediately after compaction, any molds with an exposed surface were placed under wet hessian sheets to provide a moist environment for curing. All samples were stored in the concrete laboratory for 23 ± 2 hours. After this time, they were demolded and transferred to curing tanks. To avoid cross-contamination, samples from different mixes were cured separately in lime-saturated water, at a standard tropical zone temperature of 27 ± 2 °C until the appropriate testing age.

2.3 Sample preparation and testing procedure

2.3.1 Fresh properties

The water demands for normal consistency and setting time for the cement with five different dosages of calcium nitrite (0%, 1%, 2%, 3% and 4%) were tested on cement pastes in accordance with AS/NZS 2350.4 [30]. Slump tests and plastic density tests were conducted on fresh concrete immediately after mixing according to AS 1012.3.1 [31].

2.3.2 Compressive strength

Compressive strength tests were carried out on the concrete in accordance with AS 1012.9 [32], using cylindrical molds of dimensions Ø100 x 200 mm. Three cylinders from each mix were cast as mentioned in section 2.2 and used for the compressive strength measurements at an age of 28 days. A force was applied continuously at a rate of 20 ±2 MPa compressive stress per minute until no increase in force could be sustained, and the maximum force applied was recorded.

2.3.3 Drying shrinkages

Triplicate specimens for each concrete mix were cast in prism molds of dimensions 280 x 75 x 75 mm conforming to AS 1012.8.4 and cured as described in section 2.2 [33]. At an age of seven days from molding, samples were removed from the curing tanks, wiped with a damp cloth, and placed in a drying chamber maintained at 23 ±1°C and 50 ±5% relative humidity in accordance to AS 1012.13 [34]. The first reading was completed within 2 minutes of removing the specimen from the curing tanks. Subsequent readings were taken for each specimen, after drying periods of 7, 14, 21, 28 and 56 days.

2.3.4 The apparent volume of permeable voids

Determination of the apparent volume of permeable voids (AVPV) in hardened concrete was carried out in accordance with AS 1012.21 [35]. Test specimens were prepared by casting using Ø 100 x 200 mm test cylinders, cured as mentioned in section 2.2. Then, after up to 3mm of the top surface of each cylinder was trimmed off, each cylinder was cut into four equal slices. The slices were dried in an oven at a temperature of 105 ± 5 °C for 24 h, cooled in desiccators to a temperature of 23 ±2°C and weighed individually (M_1). Then, the specimen slices from different mixes were immersed separately in distilled water at 23 ±2 °C for not less than 48 h and then boiled for a period of 5.5 ± 0.5 h. The slices were then kept in the water until cooled to a final temperature of 23 ± 2°C and weighted individually (M_2). Each slice was then suspended on a rack and immersed in water at 23 ± 2°C and the mass was recorded as M_3. All the weight measurements were performed at an accuracy of 0.01 g. The apparent volume of permeable voids (AVPV) was calculated as:

$$AVPV = \frac{(M_2 - M_1)}{M_2 - M_3} \times 100\% \qquad (1)$$

2.4 Leaching of nitrite from admixed concrete

The test methodology generally followed the specifications of ANSI/ANS- 16.1-1986 [36]. Triplicate specimens from each calcium nitrite dosage (1%, 2%, 3%) were cast using cylindrical molds of dimensions Ø 40 x 40 mm and cured individually in one-liter lime-saturated water at standard tropical zone temperature of 27 ± 2 °C for 28 days. After curing, each cylinder was placed, supported by a plastic stand, inside a lidded plastic container with 800 mL deionized water (DI) at 24±0.5°C. The DI water maintains a uniform thickness around the specimen providing a ratio of liquid solution volume to specimen surface area at 12.7 cm.

The leached solution was sampled and completely replaced by fresh DI water at regular intervals during cumulative leaching times ranging from 2 to 10320 h (over 430 days). For analysis of the leached nitrite concentration, 5 mL of leached solution was filtered (0.22 mm membrane) and analyzed using a Lachat QuikChem 8000 (Milwaukee) flow-injection analyzer (FIA). To assess the leaching process, a cumulative fraction leached (CFL) was defined as the sum of the fractions of nitrite leached during all sampling intervals prior to and including the present interval divided by the amount of nitrite in the test specimen before the test. For the i-th liquid replenishment, the CFL was calculated as

$$CFL = \sum_{i=1}^{n} \frac{a_i}{A_0} \quad (2)$$

where A_0 is the total amount of nitrite inside the specimen at the beginning of the leaching experiment, which was calculated as the nominal admixed amount. And a_i is the leached amount of nitrite at the i-th liquid replenishment interval.

2.5 Biofilm development in wastewater and microbial community analysis

Triplicate cylinders were cast with a diameter Ø 2 cm x 3 cm using the mortar from each of 0%, 2% and 4% calcium nitrite mixes with coarse aggregates removed by a 4.75 mm sieve. After casting, the specimens were cured as mentioned in section 2.2 for 28 days. Then, cylinders from each mix level were clustered on stainless-steel rods using cable ties and transferred to a lab-scale rising main sewer reactor (Figure S1) to simulate the anaerobic conditions in real sewers. Three reactors, made of Perspex with a volume of 0.75 L, were built to provide a similar ratio of liquid solution volume to specimen surfaces area as leaching tests in section 2.4.

Domestic wastewater collected weekly from a nearby wet well in Brisbane, Australia, was stored in a cold room at 4 °C, and used as the feed to the reactors. The sewage typically contained sulfide at concentrations of <3 mg-S/L, sulfate at 10-25 mg-S/L, total chemical oxygen demand (COD) and soluble COD at 450-600 mg/L and 260-450 mg/L, respectively, with the latter including volatile fatty acids (VFAs) at 50-120 mg-COD/L. The hydraulic retention time (HRT) of the reactors was maintained as 6 hours, a common HRT in sewers. The wastewater was preheated to room temperature before being pumped into the reactors through a peristaltic pump (Masterflex 7520-47). Each pumping event lasted 4 min for every 6 hours at the flow rate of 275 mL/min. Constant mixing was provided at 250 rpm with a magnetic stirrer (Heidolph MR3000) to produce a moderate shear force at the inner surface of the reactor wall.

After 3 and 6 months of incubation, one cylinder from each type of concrete was removed from the reactor. The biofilm attached on the surface of each cylinder was collected using a sterile surgical scalpel into a sterile 50 mL polypropylene falcon tube and stored at 4 °C for less than 24 h before DNA was extracted.

The DNA was extracted from the biofilm samples using the Fast DNA™ SPIN Kit for Soil (MP Biomedicals, CA, USA), as per manufacturer's instructions. The extracted DNA samples were provided to the Australia Center for Ecogenomics (ACE, Brisbane, Australia) for 16S rRNA gene amplicon sequencing (Illumina). The extracted 16S rRNA gene was amplified using the universal primer set 926F (5'- AAACTYAAAKGAATTGACGG-3') and 1392R (5'-ACGGGCGGTGTGTRC-3'). The resulting PCR amplicons were purified using Agencourt AMPure XP beads (Beckman Coulter). Then the purified DNA was indexed using the Illumina Nextera XT 384 sample Index Kit A-D (Illumina FC-131-1002) in standard PCR conditions with Q5 Hot Start High-Fidelity2X Master Mix. After that, Amplicons were pooled in equimolar concentration and sequenced with an Illumina sequencer (MiSeq Sequencing System) based on the standard protocols.

Raw sequencing data were quality-filtered and demultiplexed using Trimmomatic, with poor-quality sequences trimmed and removed. Subsequently, high-quality sequences at 97%

similarity were clustered into operational taxonomic units (OTUs) using QIIME with default parameters, and representative OTU sequences were taxonomically BLASTed against Greengenes 16S rRNA database. Finally, an OTU table consisting of the taxonomic classification and OTU representative sequences was used to analyze the microbial community structure.

2.6 Linear regression models for accessing the impact of calcium nitrite dosages

Linear regression analysis was performed on the properties of the paste or concrete including setting time, w/c for normal consistency, slump, density, compressive strength, drying shrinkage and apparent volume of permeable voids (AVPV) against calcium nitrite dosages using R (ver 3.31, http://www.R-project.org/). The linear regression typically generates the correlation in terms of a straight line which best approximates all the individual data points including target and output parameters [37]. The general form of the linear regression is given as equation 3:

$$\hat{Y} = a_0 + \mathrm{b}_0 \mathrm{n} \quad (2)$$

Where $\hat{Y}$ is the model's output, n is the calcium nitrite dosage (%), and a_0, b_0 are the regression coefficients.

For each property, the significance of the non-zero slope was analyzed using F-test by the *p* value. Then the linear regression models were built based on the data points obtained under 5 different dosages (i.e. 0, 1, 2, 3, 4) for the properties with significant non-zero slopes. The coefficients of determination (R^2) were employed as the indicator to assess the performance of linear regression models.

3 Results and discussion:

3.1 Setting time and water demand for normal consistency

Since setting time is related to the handling time of fresh concrete, a proper dosage is critical for the use of calcium nitrite in industrial and commercial applications. In sulfate-resistant cement pastes, the initial setting time and final setting time decreased due to the addition of calcium nitrite (Figure 1A). With higher calcium nitrite dosages, higher reductions of initial setting times and final setting times were observed (Figure 1A). In comparison to the control without calcium nitrite, 42% and 36% reduction in the mix with 1% calcium nitrite and 58% and 42% reduction in the mix with 2% calcium nitrite were observed for the initial and final setting time, respectively. In previous studies using OPC, the addition of calcium nitrite at 1% by weight, led to 31% and 16% reduction and 2% addition led to 65% and 44% reduction, in initial setting time and final setting time, respectively [21]. In comparison to those previous reports, the different reduction ratios in this current study might be caused by the different cement types. However, a higher accelerating effect due to a higher calcium nitrite dosage were observed in this current study and previous studies. In this study, for the mix with 4% calcium nitrite, the initial setting time and final setting time dropped to *c.a.* 18 minutes and *c.a.* 41 minutes, respectively. Based on the current mix design in this study, the higher nitrite dosage (>4%) would lead to a very short and impractical setting time.

Through the linear regression analysis, no-zero slopes were confirmed for both initial setting (p= 0.0067) and final setting time (p=0.0060), respectively. Linear regression models were established for both initial setting time (t_i, minutes) and final setting time (t_f, minutes), with the admixed level of calcium nitrite (n, %) (Figure 1A). The good fitting performance of these models (R^2=0.94 in both cases) suggests the potential of using the linear regression models for optimizing the calcium nitrite dosage and operational procedure for specified setting time.

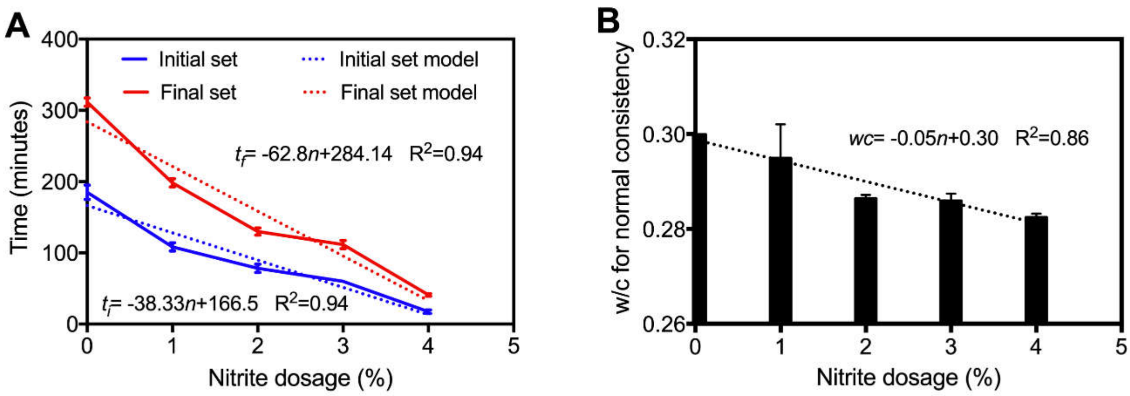

Figure 1 Setting time of cement pastes with various nitrite dosages (A); water/cement ratio for normal consistency of cement pastes under 5 dosages of calcium nitrite (B).

The w/c needed for normal consistency of control mix (0% calcium nitrite dosage) is similar to that in OPC [38]. The addition of calcium nitrite significantly reduced the water demand of the mix. For the 4% calcium nitrite admixed mix, the w/c needed for normal consistency was reduced from *c.a.* 0.30 to *c.a.* 0.28, compared with the control mix. This suggests that less water is required for a desired consistency with the addition of calcium nitrite. The water demand is one of the most important criteria for mix design, which affects the fresh and hardened properties of concrete [39]. Through linear regression analysis, a non-zero slope was confirmed (p=0.024). The linear regression model (R^2 =0.86) can be employed to adequately determine the w/c for different admixture levels of calcium nitrite (Figure 1B).

3.2 Slump and density

The slump of fresh concrete significantly increased with the calcium nitrite addition (Figure 2). Compared with control (0% calcium nitrite), the slump of 4% mix increased from *c.a.* 143 mm to *c.a.* 253 mm. Previously, slump increases from 75 mm to 95 mm and 55 mm to 90 mm, in OPC and blast furnace slag cement, with the addition of around 1.8% calcium nitrite by mass of cement, are reported respectively [23]. Another study found that the slump increased from 66 mm to 91 mm in OPC with the addition of 2% of calcium nitrite by the mass of cement [21]. The observation in this study is consistent with previous reports. Furthermore, the relationship between different calcium nitrite dosages and the slump has been clearly identified in this study.

A significant non-zero linear slope was confirmed between the level of calcium nitrite (n, %) and the average slump (*Slump*) through linear regression analysis (p=0.049), and the linear regression model described the relationship well (R^2 = 0.78) (Figure 2). This coincides with the linear decreasing trend in the water demand of cement paste to achieve a normal consistency under different calcium nitrite dosages (section 3.1). Since there are different methods for constructing concrete pipes and each method requires different workability, there is no specific limitation for the slump in the Australian standard for sewage-related infrastructures [13]. The slump values measured in this study for all five mixes are within the range of normal weighted aggregate concrete [40]. Consistent with the reduced water demand, to achieve a fixed slump, less water will be required for the concrete with calcium nitrite as an admixture.

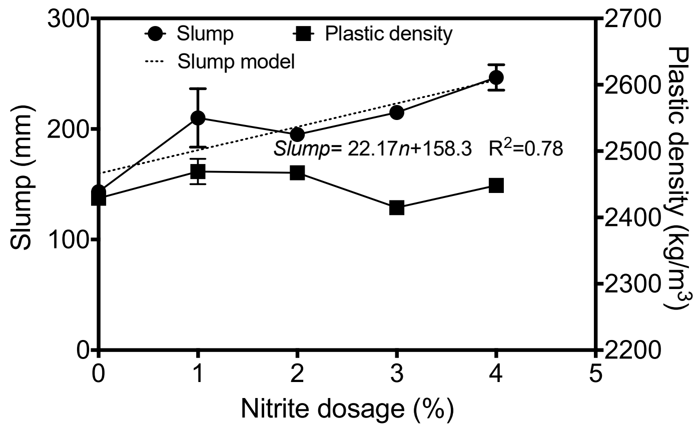

Figure 2 Slump and plastic density of concrete with various nitrite levels

Through linear regression analysis, a non-zero slope between plastic density and nitrite dosage was not significant (p=0.86). Limited variations in plastic density were observed between mixes of different calcium nitrite levels (Figure 2), suggesting that the plastic density was not significantly affected by calcium nitrite addition and its dosage. The plastic density of the 3% calcium nitrite mix was slightly lower than other mixes, and this is likely caused by the higher air content in the 3% fresh mix. The higher air content in the 3% mix, in turn, was most likely due to incomplete consolidation resulting from accelerated setting. The plastic density of all five mixes was between 2400 kg/m^3 to 2500 kg/m^3, which is equivalent to that of conventional concrete [41].

3.3 Compressive strength and hardened density

For most sewer concrete, 50 MPa is the minimum 28-day cylinder compressive strength requirement and this was achieved for all the sulfate-resistant concrete with added calcium nitrite at 0%, 1%, 2%, 3% and 4% (Figure 3). Due to calcium nitrite admixing, the compressive strength increased in most of the previous studies [21, 23]. However, in some recent studies, calcium nitrite showed an adverse impact on the compressive strength at the later stage of curing, which might be attributed to the increase of micropore size during the hydration process [22]. Through the linear regression analysis, the slope between 28-day compressive strength and calcium nitrite dosage was not significantly non-zero (p=0.96), suggesting the insignificant impact of calcium nitrite addition on the 28-day compressive strength of concrete. The observation is consistent with some previous studies [42, 43]. Since the concrete type, curing condition, calcium nitrite dosage and types of other admixtures are different in each study, the observation about the insignificant change of compressive strength might be limited to the current mix design and curing condition.

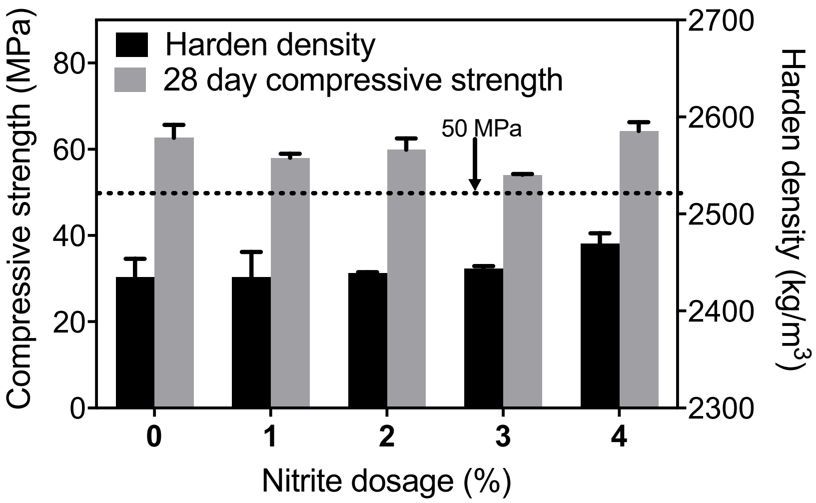

Figure 3 Compressive strength and hardened density of concrete under five calcium nitrite dosages

The hardened density of all the mixes was in the range of 2400-2500 kg/m^3, which is similar to most of the concrete manufactured with OPC [23]. Although there is a slight increase of hardened density with a higher nitrite dosage, the non-zero slope between hardened density and calcium nitrite dosage was insignificant (p=0.07) (similar to the plastic density) and variations observed between mixes of different calcium nitrite levels are limited (Figure 3).

3.4 Drying shrinkage and permeable voids

The addition of calcium nitrite increased the drying shrinkage and higher shrinkage was observed with higher doses of calcium nitrite (Figure 4A). Through the linear regression analysis, the non-zero slope between drying shrinkage and calcium nitrite dosage gradually became significant with p values decreasing from 0.063 at day 7 to 0.045 at day 28, and 0.030 at day 56 (Table S1). In hardened concrete, drying shrinkage is the volume of water lost from hardened concrete stored in unsaturated air [44]. The increased drying shrinkage especially at later stages (after 21 days), suggested a higher volume of water loss from concrete due to a higher calcium nitrite dosage. The water lost during drying shrinkage is the excess from the mix which does not react with the cement, but is required to aid compaction and workability, and becomes trapped in the pores of the hardened cement paste [45]. As discussed in section

3.1, the calcium nitrite addition reduced the water demand for cement paste, which in turn increased the volume of water that was lost from hardened concrete samples at constant w/c in drying shrinkage tests. In addition, due to the acceleration effect caused by calcium nitrite, a more porous microstructure of cement paste is likely to be formed during the hydration process, which would increase the volume of water loss during the drying shrinkage testes[22].

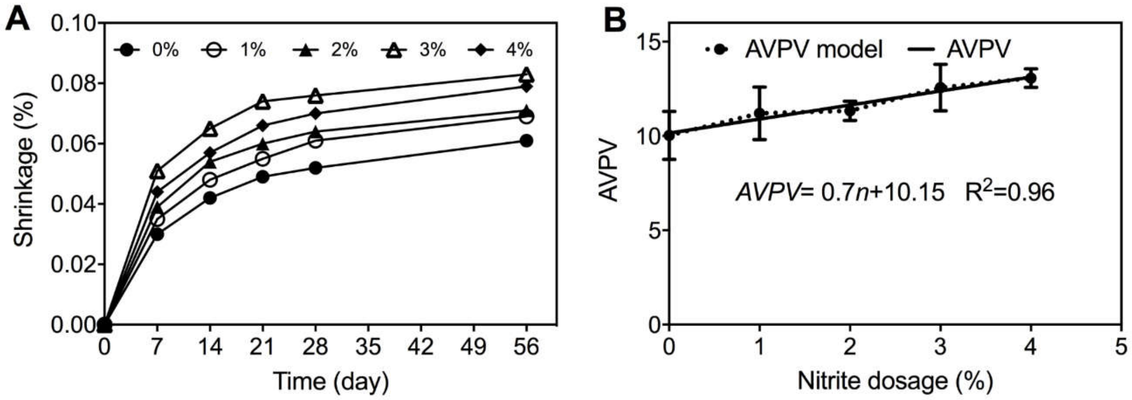

Figure 4 Drying shrinkage (A) and apparent volume of permeable voids (AVPV) (B) of concrete with different calcium nitrite dosages

The drying shrinkage observed at day 56 for all five mixes were within a range of 0.061% to 0.083%. Such results are in line with previous studies where calcium nitrite has been used as an admixture [46, 47]. There is no specific requirement for wastewater infrastructures in Australia regarding drying shrinkage. However, according to the standard regarding concrete structures for retaining liquids, the drying shrinkage measured in 56 days should be less than 0.07% [13]. The drying shrinkage of mixes with 3% and 4% of calcium nitrite were just above this limit. Due to the evaporation of free water in capillary pores, drying shrinkage occurs and this induces the transport of water particles from calcium silicate hydrates (C-S-H) to the capillary pores. This circumstance produces internal stress, mass loss and consequently volume reduction of the concrete and becomes one of the main causes for the cracking of restrained concrete [48]. In this study, the higher drying shrinkage due to calcium nitrite addition may increase the potential of cracking. Therefore, for better durability, the dosage of calcium nitrite should be optimized to prevent the adverse effects of shrinkage.

For the apparent volume of permeable voids (AVPV), the addition of calcium nitrite increased AVPV in a linear pattern. Through linear regression analysis, the non-zero slope between AVPV and calcium nitrite dosages (n, %) was significant (p=0.0036), and the linear regression model described the data well (R^2 = 0.96) (Figure 4B). The AVPV in hardened concrete is affected by the extra water added in the mix since it increases the capillary porosity of concrete [49]. The linear increase of AVPV with increased calcium nitrite additions is consistent with the reduced water demand for cement paste (section 3.1) and increased drying shrinkage detected at the higher doses.

The AVPV increased from 10.0% in the control mix (0% calcium nitrite) to 13.1% in the 4% calcium nitrite mix. The AVPV observed for control mix is similar to most of the OPC concrete and fly ash blended concrete [50, 51]. For wastewater infrastructures, the increased AVPV would provide increased access of chloride and sulfate ingress, which may accelerate both steel and concrete corrosion. In addition, although there is no specific requirement for sewage-related infrastructures regarding AVPV, a concrete with AVPV values less than 13% is generally classified as good-quality concrete for bridges and roads [52]. For the mixes with calcium nitrite dosages lower than 4%, the AVPV were all below this limit, suggesting limited pore interconnectivity in the concrete. Extra care should be taken on 4% calcium nitrite mix since the AVPV is slightly higher than the general limit.

The AVPV and drying shrinkage results suggest that the addition of calcium nitrite affects the cement paste microstructure – possibly increasing the number or size of pores in the cement paste (Figure S2). The pore structures have been reported to affect the compressive strength, where a lower compressive strength is observed in concrete with a higher volume of pore structures [22]. However, the compressive strength in this study was not affected by the nitrite admixture (section 3.3).

3.5 Leaching of nitrite from admixed concrete

The cumulative fraction of leached (CFL) nitrite from concrete cylinders with nitrite is reported to be proportional to the square root of leaching time [25]. Therefore, the CFL of the concrete with 1%, 2% and 3% calcium nitrite were calculated as functions of $t^{0.5}$ in Figure 5. Except for an initial transient region, an approximately linear correlation between the CFL and $t^{0.5}$ is evident for each specimen, which indicates that the leaching of nitrite is dominated by diffusion [53]. The relative slower leaching rate during the initial transient period is commonly observed in cylinders with casting surfaces [25, 54]. This is attributed to the relatively lower nitrite concentration near the concrete surface than the bulk concrete, which was caused by nitrite loss during the curing.

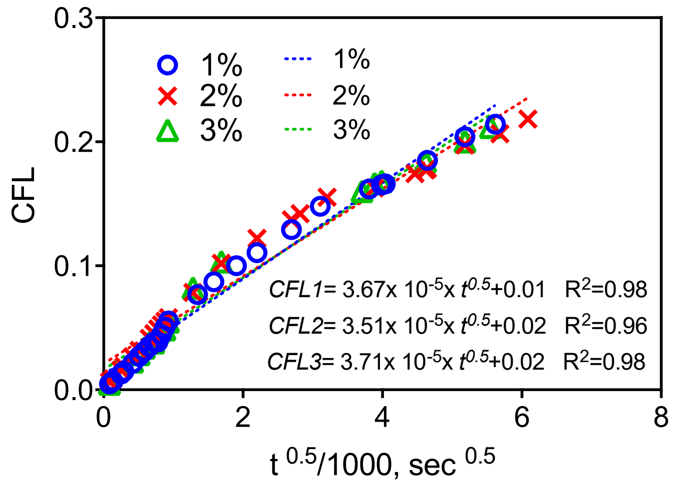

Figure 5 Cumulative fraction leached (CFL) of concrete with 1%, 2% and 3% calcium nitrite as an admixture.

The slopes of CFL versus $t^{0.5}$ for all three dosages are similar, suggesting that the dosage level doesn't affect the leaching performance in terms of CFL. The slopes ranged from 3.51×10^{-5} $sec^{-0.5}$ to 3.71×10^{-5} $sec^{-0.5}$ for all three mixes, which is at the same magnitude determined in previous reports using concrete cylinders [25]. The similar slope observed for all these three mixes suggests that in receiving water, the concentration of nitrite leached is linearly proportional to the nitrite dosage in concrete. Therefore, a higher dosage of calcium nitrite in concrete can induce a higher nitrite concentration in receiving water system, which may affect the biofilm development in wastewater infrastructures.

3.6 Biofilm development on nitrite admixed concrete in wastewater

The microbial communities were determined for biofilms developed on control coupons (0%), and 2%, and 4% calcium nitrite admixed coupons after being incubated in wastewater for 3 months (N0M3, N2M3, N4M3) and 6 months (N0M6, N2M6, N4M6). The microbial development on control coupons represents the normal concrete condition in the sewer environment. Shannon index is widely used as an indicator for the alpha diversity of samples, to describe the richness and evenness of microbial data [55]. The Shannon index observed for all the coupons was 4.80-5.35, which is similar to that previously observed in sewer biofilms [56]. As shown in Figure 6, *Desulfovibrio*, *Blvii28 wastewater-sludge group*, *Methanospirillum*, *Paludibacter*, *Smithella*, *Caldisericum*, *vadinBC27 wastewater-sludge group*, and *Methanosaeta* were found to be the top eight genera of microbes in the aspect of abundance. All these microbes are commonly detected in anaerobic wastewater [26, 57-59]. *Desulfovibrio* is a typical sulfate-reducing bacteria (SRB) that produces sulfide in the anaerobic parts of sewer facilities [26]. The phylum *Latescibacteria* is detected in the intestinal tracts of insects and is potentially relevant for organic removal in wastewater treatment [59]. *Paludibacter* and *Caldisericum* are found in wastewater-related reactors and have the ability of reducing sulfur compounds to sulfide in wastewater [57, 60]. *Methanosaeta* and *Methanospirillum* are methanogens, which are likely facilitating methane production [58]. Bacteria of the genus *Smithella* are propionate-oxidizing anaerobes that rely on syntrophic association with methanogens [58].

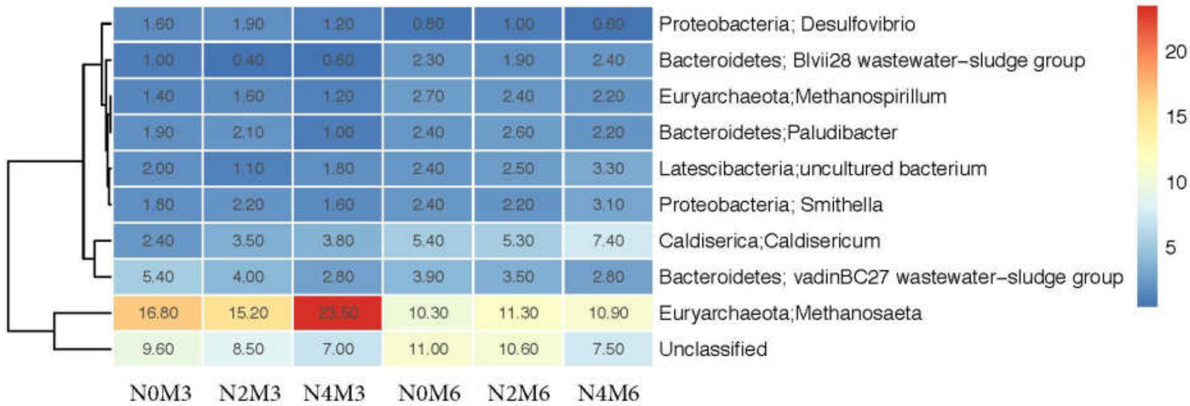

Figure 6 Heatmap summarizing the relative abundances of bacteria (each row representing an OTU) in the biofilms collected from the surface of control coupons (0%), and on 2%, and 4% calcium nitrite admixed coupons after being incubated in wastewater for 3 months (N0M3, N2M3, N4M3) and 6 months (N0M6, N2M6, N4M6). The relative abundance is defined as a percentage in total effective microbial sequences in a sample. Reads that could not be classified are collectively referred to as 'unclassified'.

From the 3rd month to 6th month, the Shannon index of each coupon decreased slightly, from 5.35 to 5.02, from 5.30 to 5.16 and from 5.33 to 4.80 for the control, 2%, and 4% calcium nitrite coupons, respectively. The relative abundance increased for most of the microbes including *Blvii28 wastewater-sludge group*, *Methanospirillum*, *Paludibacter*, *Smithella*, *Caldisericum* and the phylum *Latescibacteria* after 6-month incubation. This observation is consistent with the reduction of the Shannon index, suggesting the reduced diversity of biofilms and the stabilization of abundant microbes [56]. After the same incubation time (3 months or 6 months), the Shannon index of nitrite coupons were lower than the control coupons. This implies that nitrite in concrete is a selective factor influencing the microbes that grow on the surface of admixed concrete.

After the first three months, the relative abundances of *Caldisericum* on nitrite coupons were 45.8% and 58.3% higher for N2M3 and N4M3, respectively, compared with control coupons. Similarly, after 6 months of incubation, the relative abundance of *Caldisericum* was still 19.2% higher on N4M6 than the control. The genus *Caldisericum* contains only a sole cultured species, *Caldisericum exile*, isolated from a hot spring. The isolate is characterized as sulfur-reducing bacteria (SRB), which can reduce thiosulfate and elemental sulfur but not sulfate [61]. Some SRB are reported to have a nitrite reductase as a detoxification mechanism to survive in environments containing nitrite [62]. However, the gene for this nitrite reductase was not evident on the genome of *Caldisericum exile*. The reason for the increased relative abundance of this SRB in the presence of nitrite is not evident. However, in a previous study, nitrite is seen to stimulate biological sulfide oxidation within a sewer biofilm under anaerobic conditions [63]. This causes increases in the formation of the intermediate sulfur compounds elemental sulfur and thiosulfate, through the partial oxidation of sulfide [63]. Thus, a possibility here is that the increased abundance of *Caldisericum,* in the presence of released nitrite, is related to the increased availability of these intermediate sulfur-based substrates.

The relative abundance of *Methanosaeta* on N4M3 was 40.5% higher than the control biofilm. In some recent studies, *Methanosaeta* is found as the dominant methanogen in anaerobic reactors with nitrite, where methanogenesis and denitrification were simultaneously occurring [64]. This suggesting that *Methanosaeta* has some tolerance to nitrite, leading to its increased abundance in N4M3. However, after the longer incubation, the impact of nitrite on the abundance of *Methanosaeta* became insignificant (N4M6).

No significant difference was detected between control coupons and nitrite coupons for the relative abundance of *Desulfovibrio*, *Methanospirillum*, *Paludibacter*, *Latescibacteria* and *Smithella* after the 3 and 6 month incubations. In previous studies, the biocidal/inhibitory effect of nitrite for SRB and methanogens has been observed in sewer biofilms due to the formation of free nitrous acid (FNA), the protonated form of nitrite [65, 66]. For SRB and methanogens, at parts per billion (ppb) level, FNA inhibits the microbial metabolism and becomes a strong biocidal agent, at parts per million ppm levels [65, 66]. Based on the leaching performance of nitrite (section 3.6), the maximum concentration of FNA in wastewater (pH=7) is excepted to be around 0.24 ppb and 0.48 ppb for 2% and 4% coupons respectively. The microbial community analysis of coupon biofilms suggests that these levels of FNA had no inhibitory effect on the SRB and methanogens. In contrast, the presence of *Caldisericum* was temporarily stimulated in the nitrite admixed concrete, possibly due to the formation of thiosulfate and elemental sulfur through nitrite oxidation of sulfide [67]. Overall, the influence of the nitrite admixture in concrete on the long-term development of sewer biofilms was negligible.

3. Conclusion:

This study investigated the feasibility of adding calcium nitrite as an admixture into sulfate resistant cement for wastewater structures. Based on the results, the following conclusions are drawn:

- The addition of calcium nitrite increased the setting time of paste, the slump, the drying shrinkage, and the AVPV of sulfate-resistant concrete. The addition reduced the water demand of the paste to achieve normal consistency. The properties of paste and concrete change with calcium nitrite dosages were linear relationships. A nitrite dosage of less than 4% is recommended to minimize the negative impacts on concrete mechanical properties.
- The compressive strength, the plastic density and the hardened density of concrete were not affected by calcium nitrite addition and they meet the requirement to be used for wastewater structures.

- The cumulative fraction of leached nitrite is dominated by diffusion, which can be described as a linear function of $t^{0.5}$. The CFL is independent of the dosage of calcium nitrite.
- The microbial community on admixed concrete surfaces reached comparable states to non-admixed concrete after 6 months, although some SRB such as *Caldisericum* was temporarily stimulated by nitrite from admixed concrete in sewage cultivation.

Acknowledgements:

The authors acknowledge the financial support provided by the Australian Research Council and the following partners: Gold Coast Water and Waste, District of Columbia Water and Sewer Authority, South East Water for their support through the Australian Research Council Linkage Project LP150101337. Dr. Guangming Jiang is the recipient of an Australian Research Council DECRA Fellowship (DE170100694). Xuan Li acknowledges the Chinese Scholarship Council for providing the Living Allowance Scholarship.

Data availability

The raw/processed data required to reproduce these findings cannot be shared at this time as the data also forms part of an ongoing study.

References:

[1] T.A. Söylev, M. Richardson, Corrosion inhibitors for steel in concrete: State of the art report, Construction and Building Materials, 22 (2008) 609-622.

[2] J. Sulikowski, J. Kozubal, The durability of a concrete sewer pipeline under deterioration by sulphate and chloride corrosion, Procedia Engineering, 153 (2016) 698-705.

[3] G. Jiang, J. Sun, K.R. Sharma, Z. Yuan, Corrosion and odor management in sewer systems, Current Opinion in Biotechnology, 33 (2015) 192-197.

[4] E. Bastidas-Arteaga, M. Sánchez-Silva, A. Chateauneuf, M.R. Silva, Coupled reliability model of biodeterioration, chloride ingress and cracking for reinforced concrete structures, Structural Safety, 30 (2008) 110-129.

[5] N. Delatte, Failure, distress and repair of concrete structures, Elsevier2009.

[6] G. Jiang, M. Zhou, T.H. Chiu, X. Sun, J. Keller, P.L. Bond, Wastewater-enhanced microbial corrosion of concrete sewers, Environmental Science & Technology, 50 (2016) 8084-8092.

[7] X. Li, G. Jiang, U. Kappler, P. Bond, The ecology of acidophilic microorganisms in the corroding concrete sewer environment, Frontiers in Microbiology, 8 (2017) 683.

[8] R.L. Morton, W.A. Yanko, D.W. Graham, R.G. Arnold, Relationships between metal concentrations and crown corrosion in Los Angeles County sewers, Research Journal of the Water Pollution Control Federation, (1991) 789-798.

[9] G. Jiang, E. Wightman, B.C. Donose, Z. Yuan, P.L. Bond, J. Keller, The role of iron in sulfide induced corrosion of sewer concrete, Water Research, 49 (2014) 166-174.

[10] P. Schießl, M. Raupach, Laboratory studies and calculations on the influence of crack width on chloride-induced corrosion of steel in concrete, Materials Journal, 94 (1997) 56-61.

[11] Y. Song, E. Wightman, Y. Tian, K. Jack, X. Li, H. Zhong, P.L. Bond, Z. Yuan, G. Jiang, Corrosion of reinforcing steel in concrete sewers, Science of The Total Environment, (2018).

[12] A. ACI, 211.1-Standard Practice for Selecting Proportions for Normal, Heavyweight, and Mass Concrete, 2002 (1991).

[13] AS3735-2001, Concrete structures for retainning liquids, in: T.A.W. Directory (Ed.), Australian Water Association Publications, St. Leonards, Australia, 2011.

[14] P. Chindaprasirt, P. Kanchanda, A. Sathonsaowaphak, H.T. Cao, Sulfate resistance of blended cements containing fly ash and rice husk ash, Construction and Building Materials, 21 (2007) 1356-1361.

[15] C. Shi, J. Stegemann, Acid corrosion resistance of different cementing materials, Cement and Concrete Research, 30 (2000) 803-808.

[16] R. François, S. Laurens, F. Deby, 1 - Steel Corrosion in Reinforced Concrete, in: R. François, S. Laurens, F. Deby (Eds.) Corrosion and its Consequences for Reinforced Concrete Structures, Elsevier2018, pp. 1-41.

[17] R. Leung, D. Li, W. Yu, H.K. Chui, T. Lee, M. Van Loosdrecht, G. Chen, Integration of seawater and grey water reuse to maximize alternative water resource for coastal areas: the case of the Hong Kong International Airport, Water Science and Technology, 65 (2012) 410-417.

[18] U.M. Angst, B. Elsener, C.K. Larsen, Ø. Vennesland, Chloride induced reinforcement corrosion: electrochemical monitoring of initiation stage and chloride threshold values, Corrosion Science, 53 (2011) 1451-1464.

[19] V. Ngala, C. Page, M. Page, Corrosion inhibitor systems for remedial treatment of reinforced concrete. Part 1: calcium nitrite, Corrosion Science, 44 (2002) 2073-2087.

[20] Z. Li, B. Ma, J. Peng, M. Qi, The microstructure and sulfate resistance mechanism of high-performance concrete containing CNI, Cement and Concrete Composites, 22 (2000) 369-377.

[21] N.S. Berke, A. Rosenberg, Technical review of calcium nitrite corrosion inhibitor in concrete, Transportation Research Record, (1989).

[22] A.A. Malikyar, Y. Sudoh, N. Nakajima, S. Date, Influence of calcium nitrite based accelerator, steam temperature and pre-curing time on the compressive strength of Mortar/Concrete, International Journal of Engineering and Technology, 10 (2018).

[23] G. De Schutter, L. Luo, Effect of corrosion inhibiting admixtures on concrete properties, Construction and Building Materials, 18 (2004) 483-489.

[24] M. Inoue, H. Choi, Y. Sudoh, K. Ayuta, Experimental study of leaching and penetration of nitrite ions in nitrite-type repair materials on the surface of concrete, Advances in Technology Innovation, 2 (2017) 22-24.

[25] H. Liang, L. Li, N. Poor, A. Sagüés, Nitrite diffusivity in calcium nitrite-admixed hardened concrete, Cement and Concrete Research, 33 (2003) 139-146.

[26] H. Satoh, M. Odagiri, T. Ito, S. Okabe, Microbial community structures and in situ sulfate-reducing and sulfur-oxidizing activities in biofilms developed on mortar specimens in a corroded sewer system, Water research, 43 (2009) 4729-4739.

[27] G. Jiang, O. Gutierrez, K.R. Sharma, Z. Yuan, Effects of nitrite concentration and exposure time on sulfide and methane production in sewer systems, Water Research, 44 (2010) 4241-4251.

[28] AS2972, General Purpose and Blended Cements, Standards, Australia, 2010.

[29] AS1012.2, Methods of Testing Concrete; Method 2: Preparation of the Concrete Mixes in the Laboratory, Standards Australia, Sydney, 2014.

[30] AS/NZS2350.4, Methods of testing portland, blended and masonry cement, Method 4: Setting time, Standards Australian/Standards New Zealand, 2006.

[31] AS1012.3.1, Methods of Testing Concrete, Method 3.1: Determination of properties related to the consistency of concrete - Slump test. , Standards Australian, Sydney, 2014.

[32] AS1012.9, Methods of testing concrete–Compressive strength tests–Concrete, mortar and grout specimens, SAI Global, Sydney, Standards Australian, 2014.

[33] AS1012.8.4, Methods of Testing Concrete, Method 8.4: Method of making and curing concrete - Drying shrinkage specimens prepared in the field or in the laboratory, Standards Australia, Sydney, 2015.

[34] AS1012.13, Methods of Testing Concrete; Method 13: Determination of the Drying Shrinkage of the Concrete Samples Prepared in the Field or in the Laboratory, Standards Australia, 2015.

[35] AS1012.21, Methods of testing concrete, Method 21: Determination of water absorption and apparent permeable voids in hardened concrete, Standards Australian, Sydney, 1999.

[36] ANSI/ANS-16.1, Measurement of the leachability of solidified low-level radioactive wastes by a short-term test procedure, American Nuclear Society, 1986.

[37] X. Li, F. Khademi, Y. Liu, M. Akbari, C. Wang, P.L. Bond, J. Keller, G. Jiang, Evaluation of data-driven models for predicting the service life of concrete sewer pipes subjected to corrosion, Journal of Environmental Management, 234 (2019) 431-439.

[38] A.U. Elinwa, Y.A. Mahmood, Ash from timber waste as cement replacement material, Cement and Concrete Composites, 24 (2002) 219-222.

[39] L. Turanli, B. Uzal, F. Bektas, Effect of material characteristics on the properties of blended cements containing high volumes of natural pozzolans, Cement and Concrete Research, 34 (2004) 2277-2282.

[40] J. Murata, Flow and deformation of fresh concrete, Matériaux et Construction, 17 (1984) 117-129.

[41] K. Vijai, R. Kumutha, B. Vishnuram, Effect of types of curing on strength of geopolymer concrete, International Journal of Physical Sciences, 5 (2010) 1419-1423.

[42] I. Kondratova, P. Montes, T. Bremner, Natural marine exposure results for reinforced concrete slabs with corrosion inhibitors, Cement and Concrete Composites, 25 (2003) 483-490.

[43] M.C. Brown, R.E. Weyers, M.M. Sprinkel, Effect of corrosion-inhibiting admixtures on material properties of concrete, Materials Journal, 98 (2001) 240-250.

[44] A.M. Neville, J.J. Brooks, Concrete technology, Longman Scientific & Technical England1987.

[45] W. Zhang, M. Zakaria, Y. Hama, Influence of aggregate materials characteristics on the drying shrinkage properties of mortar and concrete, Construction and Building Materials, 49 (2013) 500-510.

[46] J. Bae, N. Berke, R. Hoopes, J. Malone, Freezing and thawing resistance of concretes with shrinkage reducing admixtures, International RILEM Workshop on Frost Resistance of Concrete, RILEM Publications SARL, 2002, pp. 327-333.

[47] Z. Li, M. Qi, Z. Li, B. Ma, Crack width of high-performance concrete due to restrained shrinkage, Journal of Materials in Civil Engineering, 11 (1999) 214-223.

[48] A. Gonzalez-Corominas, M. Etxeberria, Effects of using recycled concrete aggregates on the shrinkage of high performance concrete, Construction and Building Materials, 115 (2016) 32-41.

[49] M. Olivia, P. Sarker, H. Nikraz, Water penetrability of low calcium fly ash geopolymer concrete, Proc. ICCBT2008-A, 46 (2008) 517-530.

[50] K. Pasupathy, M. Berndt, J. Sanjayan, P. Rajeev, D.S. Cheema, Durability Performance of Precast Fly Ash–Based Geopolymer Concrete under Atmospheric Exposure Conditions, Journal of Materials in Civil Engineering, 30 (2018) 04018007.

[51] M. Albitar, M.M. Ali, P. Visintin, M. Drechsler, Durability evaluation of geopolymer and conventional concretes, Construction and Building Materials, 136 (2017) 374-385.

[52] F. VicRoads, Standard Specifications for Road works and Bridge works, VicRoads Melbourne, 2006.

[53] J. Tritthart, P. Banfill, Nitrite binding in cement, Cement and concrete research, 31 (2001) 1093-1100.

[54] E. Rozière, A. Loukili, R. El Hachem, F. Grondin, Durability of concrete exposed to leaching and external sulphate attacks, Cement and Concrete Research, 39 (2009) 1188-1198.

[55] B. Wagner, G. Grunwald, G. Zerbe, S. Mikulich-Gilbertson, C. Robertson, E. Zemanick, J.K. Harris, On the use of diversity measures in longitudinal sequencing studies of microbial communities, Frontiers in microbiology, 9 (2018) 1037.

[56] P. Jin, X. Shi, G. Sun, L. Yang, Y. Cai, X.C. Wang, Co-variation between distribution of microbial communities and biological metabolization of organics in urban sewer systems, Environmental Science & Technology, 52 (2018) 1270-1279.

[57] Y. Zhang, X. Wang, M. Hu, P. Li, Effect of hydraulic retention time (HRT) on the biodegradation of trichloroethylene wastewater and anaerobic bacterial community in the UASB reactor, Applied Microbiology and Biotechnology, 99 (2015) 1977-1987.

[58] M. Sobrieraj, D. Boone, Smithella Liu, Balkwill, Aldrich, Drake and Boone 1999, 553 VP, Bergey's Manual® of Systematic Bacteriology, (2005) 1039-1040.

[59] C. Walden, F. Carbonero, W. Zhang, Assessing impacts of DNA extraction methods on next generation sequencing of water and wastewater samples, Journal of Microbiological Methods, 141 (2017) 10-16.

[60] F. Liang, Y. Xiao, F. Zhao, Effect of pH on sulfate removal from wastewater using a bioelectrochemical system, Chemical Engineering Journal, 218 (2013) 147-153.

[61] K. Mori, K. Yamaguchi, Y. Sakiyama, T. Urabe, K.-i. Suzuki, *Caldisericum exile* gen. nov., sp. nov., an anaerobic, thermophilic, filamentous bacterium of a novel bacterial phylum, *Caldiserica* phyl. nov., originally called the candidate phylum OP5, and description of *Caldisericaceae* fam. nov., *Caldisericales* ord. nov. and *Caldisericia* classis nov, International Journal of Systematic and Evolutionary Microbiology, 59 (2009) 2894-2898.

[62] S.-H. Gao, J.Y. Ho, L. Fan, D.J. Richardson, Z. Yuan, P.L. Bond, Antimicrobial effects of free nitrous acid on *Desulfovibrio vulgaris*: implications for sulfide-induced corrosion of concrete, Applied Environmental Microbiology, 82 (2016) 5563-5575.

[63] J. Mohanakrishnan, O. Gutierrez, R.L. Meyer, Z. Yuan, Nitrite effectively inhibits sulfide and methane production in a laboratory scale sewer reactor, Water research, 42 (2008) 3961-3971.

[64] T. Allegue, A. Arias, N. Fernandez-Gonzalez, F. Omil, J. Garrido, Enrichment of nitrite-dependent anaerobic methane oxidizing bacteria in a membrane bioreactor, Chemical Engineering Journal, 347 (2018) 721-730.

[65] G. Jiang, O. Gutierrez, Z. Yuan, The strong biocidal effect of free nitrous acid on anaerobic sewer biofilms, Water research, 45 (2011) 3735-3743.

[66] G. Jiang, A. Keating, S. Corrie, K. O'halloran, L. Nguyen, Z. Yuan, Dosing free nitrous acid for sulfide control in sewers: results of field trials in Australia, Water research, 47 (2013) 4331-4339.

[67] G. Jiang, K.R. Sharma, A. Guisasola, J. Keller, Z. Yuan, Sulfur transformation in rising main sewers receiving nitrate dosage, Water research, 43 (2009) 4430-4440.